Journal of Solid State Chemistry 184 (2011) 3121–3127

Contents lists available at SciVerse ScienceDirect

Journal of Solid State Chemistry

journal homepage: www.elsevier.com/locate/jssc

Two multi-dimensional frameworks constructed from zinc coordination polymers with pyridine carboxylic acids

Yuanyuan Guo, Pengtao Ma, Jingping Wang *, Jingyang Niu *

Institute of Molecular and Crystal Engineering, College of Chemistry and Chemical Engineering, Henan University, Kaifeng 475004, China

ARTICLE INFO

Article history:
Received 21 June 2011
Received in revised form
15 September 2011
Accepted 24 September 2011
Available online 4 October 2011

Keywords:
Polyoxometalate
Hydrothermal synthesis
Zinc coordination polymers

ABSTRACT

Two novel zinc coordination polymers $[Zn_2(H_2O)L(MoO_4)]_n$ (**1**) and $[Zn_4(PO_4)_2L'(H_2O)]_n$ (**2**) (H_2L=2,2′-bipyridine-6.6′-dicarboxylic acid, H_2L'=2,2′-bipyridine-4,4′-dicarboxylic acid) have been hydrothermally synthesized and characterized by elemental analyses, IR spectra, UV spectra, single-crystal X-ray diffraction and thermogravimetric analyses. Structural analyses indicate that **1** represents a 2-D sheet structure built by dimeric $[Zn_2L(H_2O)]^{2+}$ units and MoO_4^{2-} groups whereas **2** displays an interesting 3-D framework constructed by tetranuclear zinc clusters, L'^{2-} ligands and PO_4^{3-} groups. Examination of UV spectra suggests that both **1** and **2** can stably exist in the pH range of 2.45–5.45 and 3.01–8.55 in aqueous solution, respectively. The room-temperature solid-state photoluminescence of **1** and **2** are derived from the intra-ligands π–π* transitions of H_2L and H_2L' ligands and the ligand-to-metal-charge-transfer transitions.

1. Introduction

Current interest in the design and synthesis of organic–inorganic coordination polymers is not only because of their appealing structural variety but also due to their applications in optics, electronics, magnetism, catalysis and biology [1–5]. During the past decades, employing organic components to modify the crystallization of metal oxides under hydrothermal conditions to prepare novel organic–inorganic coordination polymers with unexpected structures and interesting properties has become an effective strategy [6–8]. Thus, many such coordination polymers have been obtained. For example, in 1997, Zubieta et al. reported two 1-D molybdate hybrids $[Ni(2,2'\text{-bpy})_2Mo_4O_{13}]$ and $[Cu(2,2'\text{-bpy})Mo_2O_7]$ [9], one year later, a 3-D framework $[Cu(dpe)(MoO_4)]$ constructed from $\{Cu(dpe)\}^{2+}$ linear chains bridged through MoO_4 tetrahedra was isolated by them [10]. Subsequently, Robert et al. addressed a 3-D molybdate $[Ni(dpa)_2(MoO_4)]$ [11]. In 2002, a 2-D zinc phosphate $[C_5H_{10}NH_2]_2[Zn(ZnO_2CCH_3)(PO_4)(HPO_4)]$ with four- and eight-membered apertures was obtained by Natarajan [12]. In the same year, Chandrasekhar's group communicated a tri-zinc-cluster containing phosphate $[Zn_3Cl_2(3,5\text{-}Me_2Pz)_4(t\text{-}BuPO_3)_2]$ [13]. Later, Yu and co-workers discovered a novel phosphate $(C_5H_6N_2)Zn(HPO_3)$ with left-handed and right-handed helical chains [14]. In 2005, Kruger synthesized a 2-D phosphate $\{[(bipy)Zn(H_2O)(\mu\text{-}P_2O_7)Zn(bipy)]_2\cdot 14H_2O\}$ [15]. As shown above, most of these multi-dimensional hybrid coordination polymers are constructed from transition metal cations, inorganic molybdates or phosphates and organic N-ligands. However, the reports on the multi-dimensional frameworks built up from transition metal ions, molybdates or phosphates and carboxylic acid ligands are very rare. Recently, we have launched the study on the reactions of polyoxometalate precursors and transition metal cations with carboxylic acid ligands by means of the hydrothermal technique with the aim of discovering carboxylic-participating transition metal substituted polyoxometalates based on the case that carboxylic acids have many coordination sites and can adopt flexible coordination modes, providing the excellent preconditions for creating novel high-dimensional framework architectures. During the course of investigating the reaction system containing Keggin-type $Na_2HPMo_{12}O_{40}\cdot 14H_2O$, $Zn(Ac)_2\cdot 2H_2O$ and bipyridine carboxylic acids, unexpectedly, the $Na_2HPMo_{12}O_{40}\cdot 14H_2O$ precursor decomposed into simple molybdate anions or phosphate anions, leading to the formation of two novel coordination polymers $[Zn_2(H_2O)L(MoO_4)]_n$ (H_2L=2,2′-bipyridine-6,6′-dicarboxylic acid) (**1**) and $[Zn_4(PO_4)_2L'(H_2O)]_n$ (H_2L'=2,2′-bipyridine-4,4′-dicarboxylic acid) (**2**). **1** displays a 2-D sheet structure built by dimeric $[Zn_2L(H_2O)]^{2+}$ units and MoO_4^{2-} groups whereas **2** exhibits an interesting 3-D framework constructed by tetranuclear zinc clusters, L'^{2-} ligands and PO_4^{3-} groups. The stabilities of **1** and **2** in solution have been evaluated by the in-situ UV spectra. Furthermore, the room-temperature solid-state photoluminescence properties of **1** and **2** have also been investigated.

2. Experimental

2.1. Materials and methods

All reagents were used as purchased without further purification. Elemental analyses (C, H, and N) were performed on a Perkin-Elmer 240-II CHNS/O analyzer. IR spectra were obtained

* Corresponding authors. Fax: +86 378 3886876.
E-mail addresses: jpwang@henu.edu.cn (J. Wang), jyniu@henu.edu.cn (J. Niu).

0022-4596/$ - see front matter © 2011 Elsevier Inc. All rights reserved.
doi:10.1016/j.jssc.2011.09.030

from a solid sample palletized with KBr on Nicolet FT-IR 360 spectrometer in the range of 4000–400 cm^{-1}. UV absorption spectra were obtained with a U-4100 spectrometer at room temperature. Thermogravimetric analyses were performed in N_2 on a Mettler-Toledo TGA/SDTA851^e instrument with a heating rate of 10 °C/min. Emission/excitation spectra were recorded on an F-7000 fluorescence spectrophotometer.

Table 1
Crystallographic data and structure refinements for **1** and **2**.

	1	**2**
Empirical	$C_{12}H_8MoN_2O_9Zn_2$	$C_{12}H_8N_2O_{13}P_2Zn_4$
Formula weight	550.88	711.62
T (K)	296(2)	296(2)
Crystal system	Triclinic	Orthorhombic
Space group	*P*-1	*P*2(1)2(1)2(1)
a (Å)	7.665(3)	5.0351(12)
b (Å)	9.817(4)	15.457(4)
c (Å)	10.534(4)	22.389(5)
α (deg.)	93.408(6)	90.00
β (deg.)	105.627(5)	90.00
γ (deg.)	106.728(5)	90.00
V (Å^3)	723.0(4)	1742.6(7)
Z	2	4
D_c (g cm^{-3})	2.530	2.713
μ (mm^{-1})	4.203	5.708
Crystal size (mm^3)	0.28 × 0.17 × 0.14	0.29 × 0.23 × 0.16
θ range for data collections	2.03–25.99°	1.60-25.00
Limiting indices	$-9 \le h \le 8$	$-5 \le h \le 5$
	$-7 \le k \le 12$	$-18 \le k \le 18$
	$-12 \le l \le 12$	$-23 \le l \le 26$
Reflections collected	4015	8781
Independent reflections	2793 (R_{int}=0.0127)	3036 (R_{int}=0.0286)
R_1, wR_2 [$I > 2\sigma(I)$]	0.0215, 0.0524	0.0245, 0.0524
R_1, wR_2 (all data)	0.0237, 0.0535	0.0272, 0.0530
Largest diff. peak and hole (e Å^{-3})	0.364 and −0.547	0.749 and −0.498

2.2. Synthesis

2.2.1. Synthesis of $[Zn_2(H_2O)L(MoO_4)]_n$ (**1**)

A mixture of $Na_2HPMo_{12}O_{40}\cdot 14H_2O$ (0.46 mmol, 0.87 g), $Zn(Ac)_2\cdot 2H_2O$ (3.00 mmol, 0.66 g), H_2L (0.41 mmol, 0.10 g) were successively dissolved in 10 mL HAc–NaAc buffer solution (pH= 4.8, 0.5 mol L^{-1}); the mixture was then stirred for 15 h in air, sealed in a 40 mL Telfon-lined reactor, heated at 170 °C for 10 days, and then cooled to room temperature. Colorless strip crystals were collected (yield: ca. 23% based on Mo). Elemental analyses calcd. (%) for: C, 26.16; H, 1.46; N, 5.08. Found: C, 26.13; H, 1.26; N, 5.19.

2.2.2. Synthesis of $[Zn_4(PO_4)_2L'(H_2O)]_n$ (**2**)

A mixture of $Na_2HPMo_{12}O_{40}\cdot 14H_2O$ (0.92 mmol, 1.74 g), $Zn(Ac)_2\cdot 2H_2O$ (6.00 mmol, 1.32 g), H_2L' (0.41 mmol, 0.10 g) were successively dissolved in 10 mL HAc–NaAc buffer solution (pH= 4.8, 0.5 mol L^{-1}); the mixture was then stirred for 15 h in air, sealed in a 40 mL Telfon-lined reactor, heated at 170 °C for 10 days, and then cooled to room temperature. Colorless strip crystals were collected (yield: ca. 25% based on P). Elemental analyses calcd. (%) for: C, 20.25; H, 1.13; N, 3.94. Found: C, 20.22; H, 1.16; N, 3.86.

2.3. X-ray crystallographic analysis

Intensity data for **1** and **2** were collected on a Bruker CCD Apex-II diffractometer with Mo$K\alpha$ radiation (λ=0.71073 Å) at

Table 2
Selected bond lengths (Å) and angles (deg.) for **1** and **2**.

1					
Zn1–O5	1.943(2)	Zn1–O3	2.589(2)	Zn2–O8	1.959(2)
Zn1–O1W	1.969(2)	Zn2–O2B	2.001(2)	Mo1–O5	1.777(2)
Zn1–N1	2.089(2)	Zn2–O3	1.997(2)	Mo1–O6	1.730(2)
Zn1–N2	2.126(2)	Zn2–O4A	2.186(2)	Mo1–O7	1.751(2)
Zn1–O1	2.346(2)	Zn2–O7	2.148(2)	Mo1–O8	1.767(2)
O1–C1–O1	27.2(3)	O6–Mo1–O7	109.60(11)	N1–Zn1–N2	76.97(9)
O1–C1–C2	16.2(2)	O7–Mo1–O5	110.86(10)	N1–Zn1–O1	72.02(8)
O5–Zn1–N1	110.49(9)	O5–Zn1–O1W	128.66(9)	C2–N1–Zn1	122.19(18)
O5–Zn1–N2	108.02(9)	Mo1–O5–Zn1	138.58(12)	C11–N2–C7	119.4(2)
O2–Zn2–O7	86.13(8)	Mo1–O7–Zn2	132.22(11)	C1–O2–Zn2	123.68(19)
O5–Zn1–O1	86.73(9)	Mo1–O8–Zn2	142.43(13)	C12–O3–Zn2	122.44(17)
O8–Zn2–O3	118.41(9)	Zn1–O1W–H1AW	110(3)	C1–O1–Zn1	115.52(18)
2					
Zn1–O1	1.912(3)	Zn3–O2B	1.947(3)	Zn4–O10A	2.218(3)
Zn1–O6	2.603(3)	Zn3–O3C	1.910(3)	P1–O1	1.548(3)
Zn1–O7C	1.886(3)	Zn3–O4	1.927(3)	P1–O2	1.558(3)
Zn1–N1	2.160(3)	Zn3-O11E	1.968(3)	P1–O3	1.511(3)
Zn1–N2	2.067(3)	Zn4–O6	1.972(3)	P1–O4	1.506(3)
Zn2–O1	2.306(3)	Zn4–O7C	2.636(3)	P2–O5	1.529(3)
Zn2–O2	2.008(3)	Zn4–O8B	1.985(3)	P2–O6	1.521(3)
Zn2–O5	1.920(3)	Zn4–O8C	2.054(3)	P2–O7	1.520(3)
Zn2–O12D	2.005(3)	Zn4–O9A	1.985(3)	P2–O8	1.548(3)
Zn2–O1W	2.006(3)				
O1–Zn1–N1	103.53(13)	O10–Zn4–C1	1 27.90(19)	C6–N2–Zn1	113.9(3)
O1–Zn1-N2	121.07(14)	P1–O1–Zn2	90.25(14)	C10–N2–Zn1	127.8(3)
O2–Zn2–O1	67.02(11)	P1–O1–Zn1	131.32(19)	O1–P1–O2	00.85(17)
O2–Zn3–O11	103.05(13)	P1–O2–Zn2	101.86(15)	O4–P1–O3	12.02(18)
O7–Zn1–O1	119.89(13)	P1–O2–Zn3	135.73(19)	O5–P2–O8	107.81(17)
O9–Zn4–O10	56.58(18)	P1–O3–Zn3	125.24(19)	O6–P2–O8	12.50(17)
O12–Zn2–O1	154.19(12)	P1–O4–Zn3	127.86(18)	O7–P2–O8	04.21(18)
N2–Zn1–N1	79.38(15)	P2–O5–Zn2	128.90(18)	Zn1–O1–Zn2	127.34(15)
O6–Zn4–C11	119.42(17)	C1–N1–Zn1	130.1(3)	Zn3–O2–Zn2	121.46(16)
O6–Zn4–C11	119.42(17)	C5–N1–Zn1	111.7(3)	Zn4–O8–Zn4	120.79(14)

296(2) K. Their structures were solved by direct methods and refined by full-matrix least-squares on F^2 using the SHELXTL-97 program [16]. Lorentz polarization and empirical absorption corrections were applied. Positions of the hydrogen atoms attached to carbon atoms were geometrically placed. No hydrogen atoms associated with the water molecules were located from the difference Fourier map. All hydrogen atoms were refined isotropically as a riding mode using the default SHELXL parameters. For **1**, of the 4015 reflections, 2793 unique reflections (R_{int}=0.0127) were considered and observed [$I>2\sigma(I)$]. The final cycle of refinement including atomic coordinates and the anisotropic thermal parameters converged to R_1=0.0215 and wR_2=0.0524 [$I>2\sigma(I)$]. For **2**, of the 8781 reflections, 3036 unique reflections (R_{int}=0.0286) were considered and observed [$I>2\sigma(I)$]. The final cycle of refinement including atomic coordinates and the anisotropic thermal parameters converged to R_1=0.0245 and wR_2=0.0524 [$I>2\sigma(I)$]. Crystallographic data and structure refinements for **1** and **2** are summarized in Table 1. Selected bond lengths (Å) and angles (deg.) for **1** and **2** are listed in Table 2.

3. Results and discussion

3.1. Structural description

Single crystal X-ray diffraction analyses reveal that **1** crystallizes in the triclinic space group $P-1$ and **2** crystallizes in the orthorhombic space group $P2(1)2(1)2(1)$. The molecular structural unit of **1** consists of two crystallographically unique Zn^{2+} ions, one MoO_4^{2-} anion and a L^{2-} ligand (Fig. 1a). It should be noted that two Zn^{2+} ions display two different coordination modes. The $Zn1^{2+}$ ion inhibits in the six-coordinate octahedral geometry, in which two nitrogen atoms (N1, N2) [Zn–N: 2.089(2)–2.126(2) Å] and two carboxylic oxygen atoms (O1, O3) [Zn–O: 2.346(2)–2.589(2) Å] from one L^{2-} ligand build the equatorial plane, a water (O1W) ligand [Zn–O: 1.969(2) Å] and one oxygen atom (O5) from the MoO_4^{2-} anion [Zn–O: 1.945(2) Å] occupy two polar positions. The $Zn2^{2+}$ ion adopts the trigonal bipyramid environment defined by two carboxylic oxygen atoms [O3 and O2*B* (*B*=2–*x*, 1–*y*, 2–*z*)] from two different L^{2-} ligands [Zn–O: 1.997(2)–2.001(2) Å] and one oxygen atom (O8) from a MoO_4^{2-} anion [Zn–O: 1.959(2) Å] establishing the trigonal plane and one oxygen atom (O7) from a MoO_4^{2-} anion [Zn–O: 2.148(2) Å] and a carboxylic oxygen atom [O4*A* (*A*=1–*x*, 1–*y*, 1–*z*)] from a L^{2-} ligand [Zn–O: 2.186(2) Å] standing on two apical sites. In addition, the Mo1 atom displays a tetrahedron geometry, which is bonded to four oxygen atoms [O5, O6, O7, O8*C* (*C*=2–*x*, 1–*y*, 1–*z*] with the Mo–O bond distances being from 1.729(2) to 1.776(2) Å. Meanwhile, in the skeleton of **1**, the $Zn1^{2+}$ ion is chelated by one L^{2-} ligand through two nitrogen atoms and two carboxylic oxygen atoms whereas the $Zn2^{2+}$ ion coordinates to three L^{2-} ligands via three carboxylic oxygen atoms. Adjacent two [Zn1L(H_2O)] fragments are connected together by two $Zn2^{2+}$ ions generating a dimeric $[Zn_2L(H_2O)]^{2+}$ unit. Neighboring dimeric $[Zn_2L(H_2O)]^{2+}$ units are combined with each other through two $Zn2^{2+}$ ions giving rise to the 1-D chain-like assembly (Fig. 1b). Adjacent 1-D chains are connected by MoO_4^{2-} groups forming a 2-D sheet structure (Fig. 1c). Similar 2-D framework was observed in another molybdate [Co(2,2′-bpy)Mo_3O_{10}] [9].

Different from **1**, the molecular structural unit of **2** is composed of four crystallographically unique Zn^{2+} ions, two PO_4^{3-} anions and one L'^{2-} ligand (Fig. 2d). Four Zn^{2+} ions show three kinds of coordination geometries. Both $Zn1^{2+}$ and $Zn2^{2+}$ ions adopt the trigonal bipyramid environments. The $Zn1^{2+}$ ion is defined by two oxygen atoms [O6, O7*C* (*C*=−1+*x*, *y*, *z*)] from two different PO_4^{3-} groups [Zn–O: 1.886(3)–2.603(3) Å] and one nitrogen atom (N1) from the L'^{2-} ligand [Zn–N: 2.160(3) Å] constituting the trigonal plane and one oxygen atom (O1) from one PO_4^{3-} group [Zn–O: 1.912(3) Å] and one nitrogen atom (N2) from the L'^{2-} ligand [Zn–N: 2.067(3) Å] in the axial positions. The $Zn2^{2+}$ ion is surrounded by a carboxylic oxygen atom [O12*D* (*D*=1.5–*x*, 1–*y*, −0.5+*z*)] [Zn–O: 2.005(3) Å] and an oxygen atom (O1) from one PO_4^{3-} group [Zn–O: 2.306(3) Å] and a water oxygen atom (O1W) [Zn–O: 2.006(3) Å] establishing the trigonal plane and two oxygen atoms (O2, O5) from two different PO_4^{3-} groups [Zn–O: 1.920–2.008(3) Å] standing on two apical sites (Fig. 2a). The tetrahedral $Zn3^{2+}$ ion is combined with three oxygen atoms [O4, O3*C*, O2*B* (*B*=−0.5+*x*, 1.5+*y*, 1.5–*z*)] from three different PO_4^{3-} groups [Zn–O: 1.910–1.947(3) Å] and a carboxylic oxygen

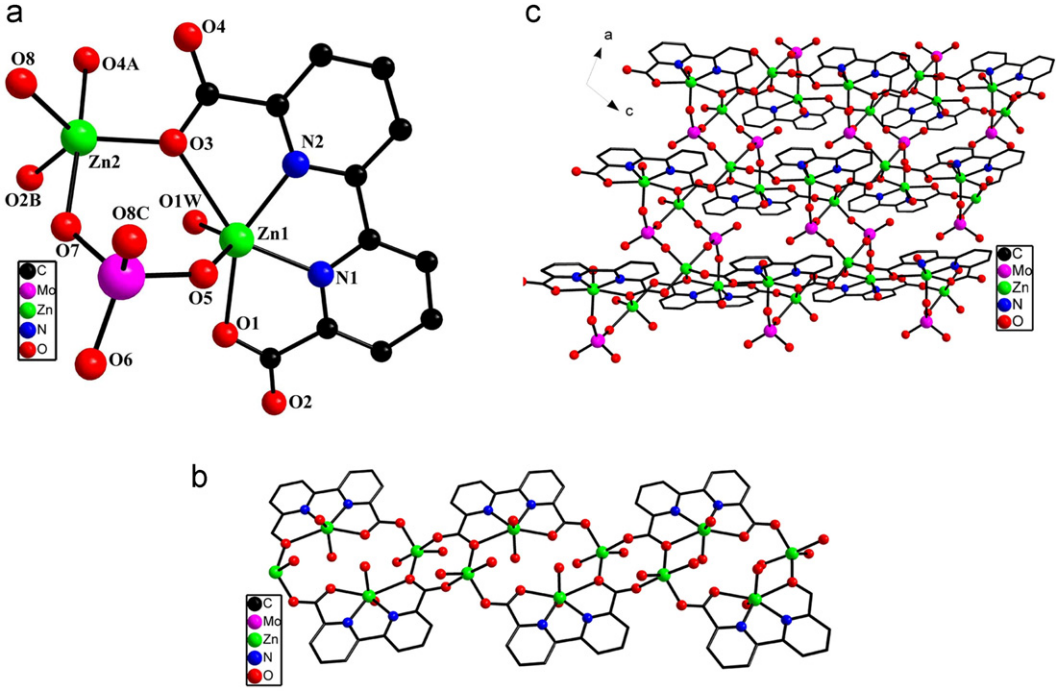

Fig. 1. (a) Ball-and-stick view of the structural unit of **1**, (b) the 1-D chain of **1** and (c) view of the 2-D sheet structure of **1**. All H atoms are omitted for clarity.

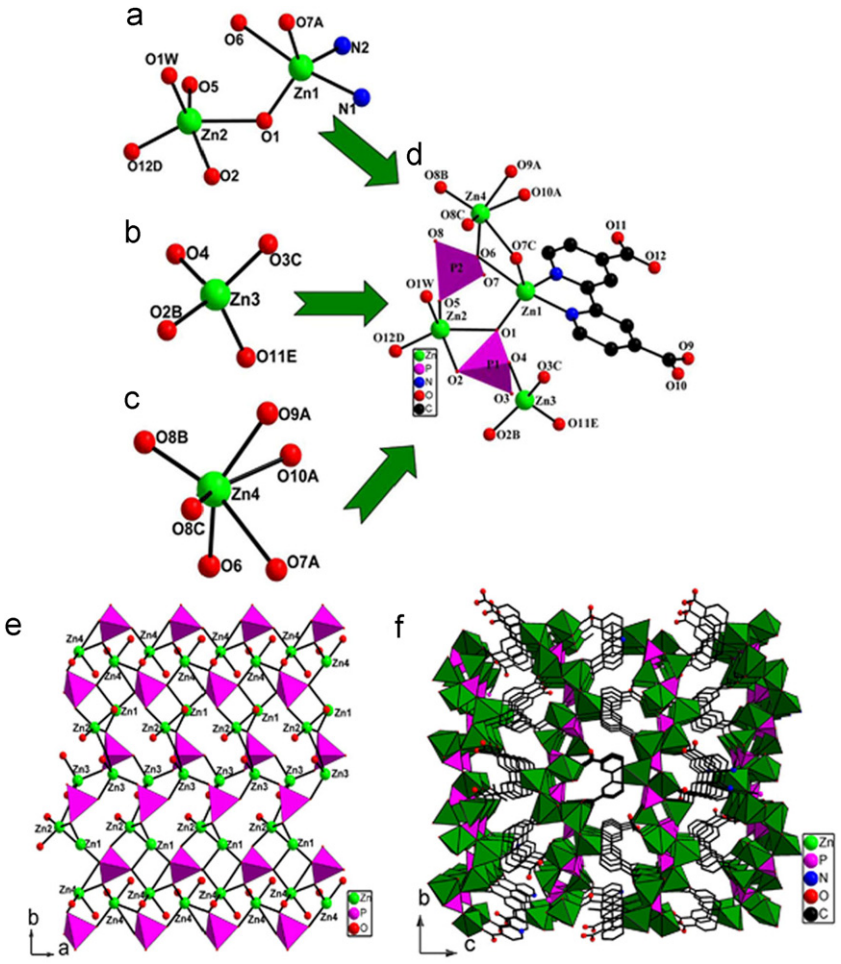

Fig. 2. (a) Coordination modes of $Zn1^{2+}$ and $Zn2^{2+}$ cations, (b) coordination mode of the $Zn3^{2+}$ cation, (c) coordination mode of the $Zn4^{2+}$ cation, (d) the polyhedral/ball-and-stick view of the structural unit of **2**, (e) 2-D sheet paralleling to the *c*-axis and (f) the 3-D framework of **2**. All H atoms are omitted for clarity.

atom [O11*E* (*E*=1–*x*, –0.5+*y*, 1.5–*z*)] [Zn–O: 1.968(3) Å] (Fig. 2b). The $Zn4^{2+}$ ion resides in a distorted octahedral geometry, which is defined by three oxygen atoms [O6, O7*C*, O8*B*] from three different PO_4^{3-} groups [Zn–O: 1.972–2.636(3) Å] and one oxygen atom [O9*A* (*A*=–*x*, 0.5+*y*, 1.5–*z*)] from one L'^{2-} ligand [Zn–O: 2.160(3) Å] building a basal plane and one oxygen atom (O8*C*) from the PO_4^{3-} group [Zn–O: 2.054(3) Å] and a oxygen atom (O10*A*) from one L'^{2-} ligand [Zn–O: 2.218(3) Å] standing on two vertexes (Fig. 2c).

It is interesting that the L'^{2-} ligand exhibits three different coordination modes: (1) two nitrogen atoms adopt the bidentate chelating coordination mode to connect one $Zn1^{2+}$ ion (Fig. 3a); (2) one carboxylic oxygen atom adopts the monodentate coordination mode to link one $Zn2^{2+}$ ion or one $Zn3^{2+}$ ion (Figs. 3b and c); (3) two carboxylic oxygen atoms act as the bidentate chelating fashion to anchor one $Zn4^{2+}$ ion (Fig. 3d). Another important feature of this structure is that the {Zn1Zn2O7} units and PO_4^{3-} groups connect with each other forming 1-D chain-like assembly. More interestingly, adjacent 1-D chains are linked together by alternate {$Zn3O_4$} tetrahedra and {$Zn4O_6$} octahedra, leading to a 2-D layer structure (Fig. 2e). The most remarkable feature of **2** is that adjacent layers are interconnected by L'^{2-} connectors forming a novel 3-D framework (Fig. 2f).

3.2. IR spectra

The IR spectrum of **1** exhibits a strong band in 920–943 cm^{-1} attributed to ν(Mo–O). The resonances in the range of 782–840 cm^{-1}

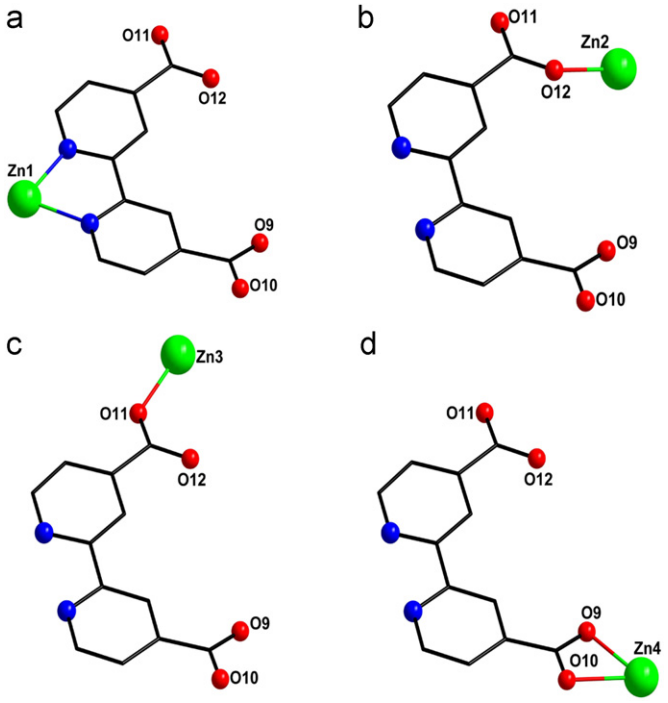

Fig. 3. Coordination modes of L'^{2-} ligand in **2**.

are tentatively assigned to ν(Zn–O–Mo). The carboxylic groups of the L^{2-} ligand are expected to give rather intense bands resulting from asymmetric (1617–1586 cm^{-1}) and symmetric (1427–1380 cm^{-1}) vibration modes [17,18]. For **2**, there are several bands between 1000 and 1023 cm^{-1} that correspond to the characteristic stretching modes of ν(P–O) [19]. Similar to **1**, the carboxylic groups of L'^{2-} are given bands resulting from asymmetric (1617–1556 cm^{-1}) and symmetric (1430–1382 cm^{-1}) vibration modes. The vibration bands in the range of 1617–1560 cm^{-1} are assigned to the anamorphic vibration of the L^{2-} ligand whereas those in the range of 1645–1430 cm^{-1} are attributed to the L'^{2-} ligand [20,21]. In addition, the weak vibration bands from 1350 to 1023 cm^{-1} are corresponded to C–N stretching modes (Fig. 4).

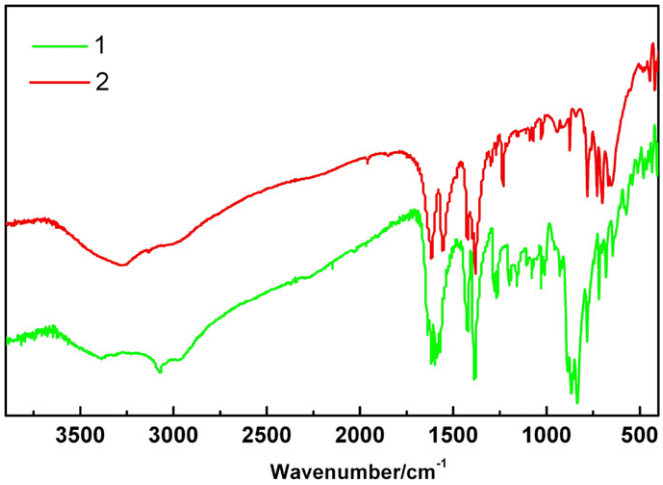

Fig. 4. Comparison of the IR spectra of **1** and **2**.

3.3. UV spectra

The UV spectrum of **1** displays a strong absorption at 218 nm and two wide shoulder absorption bands at 252 nm and 308 nm, respectively. The absorption at 218 nm can be assigned to the O→Mo charge transfer transitions [22], whereas the two absorption bands at 252 and 308 nm can be attributed to the characteristic of the L^{2-} ligand (Figs. 5a, b, and S3a). Similarly, the UV spectrum of **2** exhibits three strong absorption peaks at 210 nm, 242 nm and 311 nm, respectively. The absorption peak at 210 nm can be assigned to the charge transfer transitions of the O→Mo [22] and the absorption peaks at 242 nm and 311 nm can be attributed to the characteristic bonds of the L'^{2-} ligand (Figs. 5c, d, and S3b).

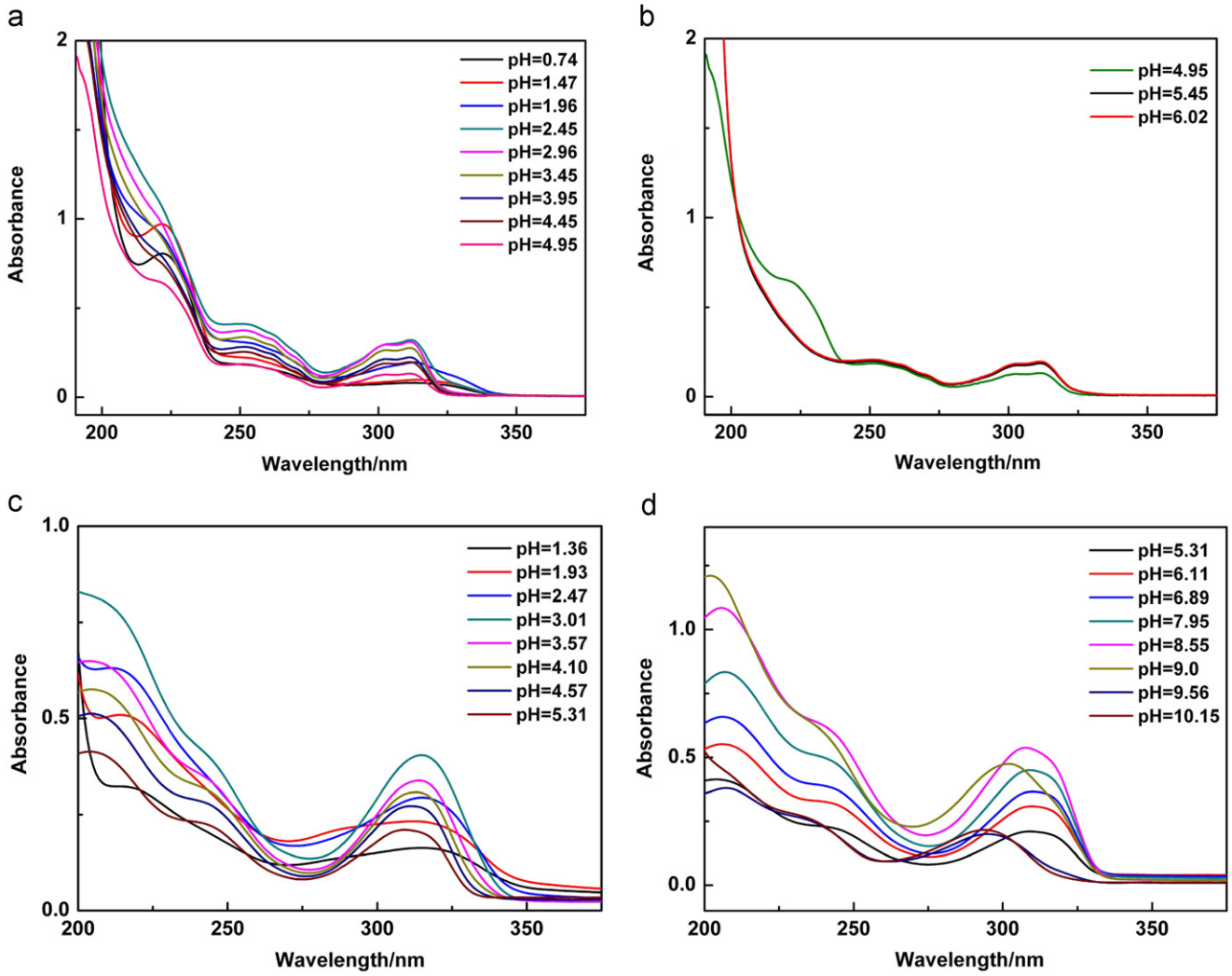

Fig. 5. Influence of the pH value on the stability of **1** and **2** in aqueous solution: (a) the UV spectral evolution in acidic direction of **1**, (b) the UV spectral evolution in alkaline direction of **1**, (c) the UV spectral evolution in acidic direction of **2** and (d) the UV spectral evolution in acidic direction of **2**.

To investigate the influence of the pH value on the stability of **1** and **2** in aqueous solution, in situ UV spectroscopic measurements of **1** and **2** were performed. The pH values in the acidic direction were adjusted using diluted HCl solution while the pH values in the alkaline direction were adjusted using diluted NaOH solution. The pH value of **1** that was dissolved in water (5×10^{-5} mol L^{-1}) was 4.95 and the UV spectrum of **1** in aqueous solution displays three absorption bands. When the pH value gradually decreases to 2.45, the change of the two shoulder absorption bands at 252 nm and 308 nm is not obvious (Fig. 5a). With the pH value further decreasing, the absorption band at 218 nm is gradually red-shifted; meanwhile the two shoulder absorption bands disappear. A conclusion can be drawn that the skeleton of **1** has been destroyed when the pH value is lower than 2.45. In contrast, when the pH value of **1** increases, the absorption band at 218 nm is weaker and weaker until vanishes (Fig. 5b), suggesting the decomposition of skeleton of **1**. The above results show **1** can stably exist in aqueous solution in the pH range of 2.45–5.45. In the case of **2**, the pH value of **2** that was dissolved in water (3×10^{-5} mol L^{-1}) was 5.31. Similarly, the pH stable range of aqueous solution of **2** is about 3.01–8.55.

3.4. Photoluminescence

Recently, the d^{10} Zn (II) compounds have attracted considerable attention on both a theoretical and a spectroscopic level because of the excellent photoluminescent properties [23]. Furthermore, the conjugated π systems containing aromatic rings are currently of interest in the development of luminescent materials [24]. As a result, the solid-state photoluminescence spectra of **1** and **2** have been investigated at room temperature (Fig. 6). It can be seen that both **1** and **2** exhibit intense emission bands at 358 and 453 nm for **1** (λ_{ex}=280 nm), and 377 nm for **2** (λ_{ex}=285 nm), respectively. On contrast, the free ligands H_2L and H_2L' display very weak emission at 352 and 381 nm for H_2L (λ_{ex}=279 nm), and 397 nm for H_2L' (λ_{ex}=276 nm), respectively (Fig. 6). The strong fluorescence efficiency of **1** and **2** is assigned to the coordination of the ligands L^{2-} and L'^{2-} ligands to the Zn (II) cations that effectively increase rigidity of the ligands and reduce the loss of energy by radiation less thermal vibrations [24]. The photoluminescence properties of **1** and **2** can be considered as the result of combination of the intra-ligands π–π* transitions of L^{2-} and L'^{2-} ligands and the ligand-to-metal-charge-transfer transitions [25].

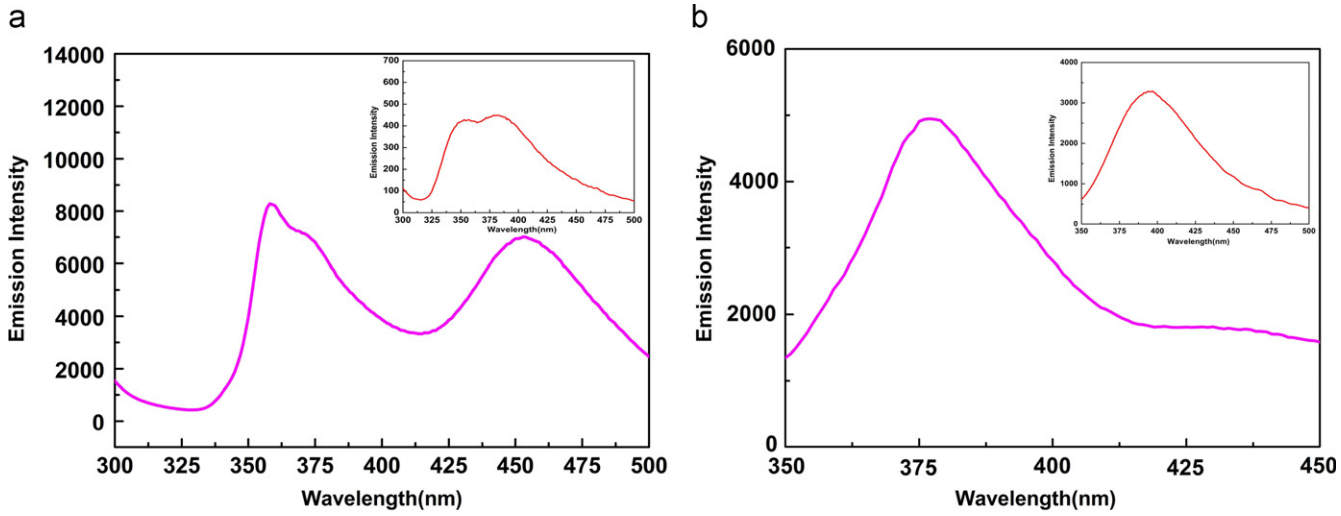

Fig. 6. Emission spectra of **1** and **2** in the solid state at room temperature.

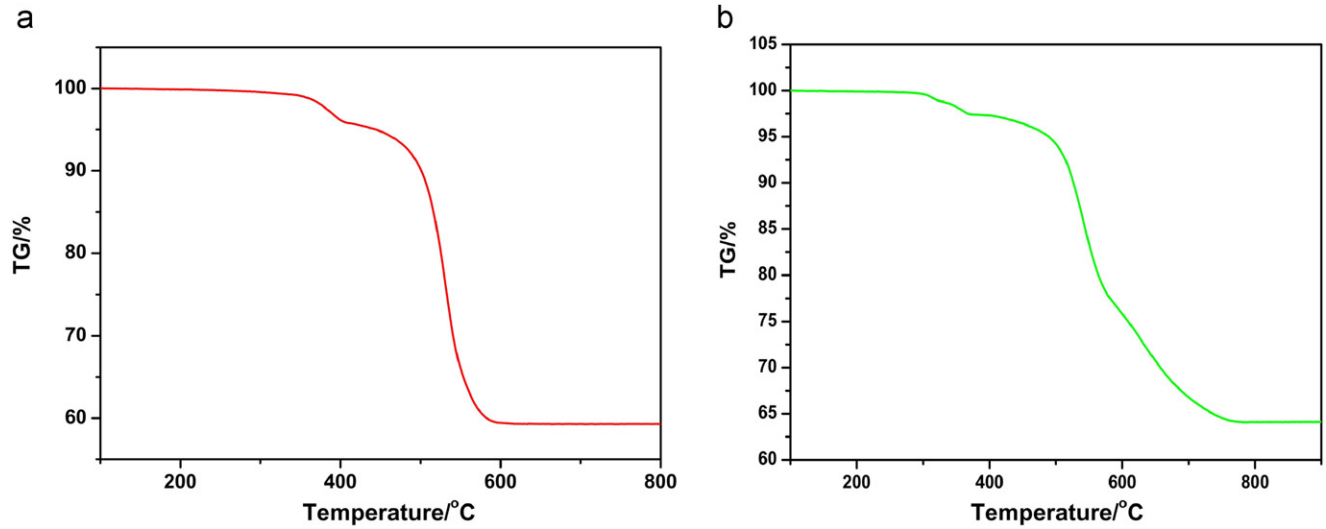

Fig. 7. Thermogravimetric curves of **1** and **2** measured under nitrogen atmosphere with a heating rate of 10 °C/min.

3.5. Thermogravimetric (TG) analyses

The TG curve of **1** exhibits two steps of weight loss in the range of 30–800 °C (Fig. 7a). The first weight loss of 3.51% between 30 and 400 °C corresponds to the release of one crystalline water molecule (calcd. 3.27%). The second stage, which occurs from 400 to 590 °C, is attributed to the loss of one organic molecule. The observed weight loss (43.52%) is in good agreement with the calculated value (43.96%). The TG curve of **2** also displays two steps of weight loss in the range of 30–900 °C (Fig. 7b). The first weight loss is 2.34% between 30 and 400 °C due to the release of one crystalline water molecule (calcd. 2.53%). The second weight loss of 31.82% between 400 and 590 °C is attributed to the removal of one organic molecule (calcd. 31.50%).

4. Conclusions

In summary, two novel zinc coordination polymers **1** and **2** have been hydrothermally synthesized and structurally characterized. **1** shows a 2-D sheet structure built by dimeric $[Zn_2L(H_2O)]^{2+}$ units and MoO_4^{2-} groups whereas **2** displays an interesting 3-D framework constructed by tetranuclear zinc clusters, L'^{2-} ligands and PO_4^{3-} groups. Examination of UV spectra suggests that both **1** and **2** can stably exist in the pH range of 2.45–5.45 and 3.01–8.55 in aqueous solution, respectively. Furthermore, the room-temperature solid-state photoluminescence of **1** and **2** are derived from the intra-ligands π–π^* transitions of H_2L and H_2L' ligands and the ligand-to-metal-charge-transfer transitions.

Acknowledgments

This work was supported by the Natural Science Foundation of China, the Foundation of Education Department of Henan Province, Natural Science Foundation of Henan Province and Natural Science Foundation of Henan University for financial support.

Appendix A. Supplementary material

Supplementary data associated with this article can be found in the online version at doi:10.1016/j.jssc.2011.09.030.

References

[1] M.T. Pope, A. Muller, Angew. Chem. Int. Ed. 30 (1991) 34–38.
[2] J. Ettedgui, R.J. Neumann, Am. Chem. Soc. 131 (2009) 4–5.
[3] P.J.S. Richardt, R.W. Gable, A.M. Bond, A.G. Wedd, Inorg. Chem. 40 (2001) 703–709.
[4] X. López, C. Bo, J.M. Poblet, J. Am. Chem. Soc. 124 (2002) 12574–12582.
[5] R. Ben-Daniel, R. Neumann, Angew. Chem. Int. Ed. 42 (2003) 92–95.
[6] Y. Toshihiro, V.P. Petra, Angew. Chem. Int. Ed. 41 (2002) 466–469.
[7] P. Mialane, C. Duboc, J. Marrot, E. Riviere, A. Dolbecq, F. Sechere, Chem. Eur. J. 12 (2006) 1950–1959.
[8] R.V. Thomas, K.S. Adam, N.S. Amy, M.O. Kang, H. Shiv, J.N. Alexander, Inorg. Chem. 45 (2006) 5529–5537.
[9] P.J. Zapf, C.J. Warren, R.C. Haushalter, J. Zubieta, Chem. Commun. (1997) 1543–1544.
[10] D. Hagrman, R.C. Haushalter, J. Zubieta, Chem. Mater. 10 (1998) 361–365.
[11] C. Matthew, L. Robert, Laskoski, Jr. LaDuca, S. Randy, Jr. Rarig, J. Zubieta, J. Chem. Soc. Dalton Trans. (1999) 3467–3472.
[12] S. Natarajan, J. Chem. Soc. Dalton Trans. (2002) 2088–2091.
[13] V. Chandrasekhar, S. Kingsley, B. Rhatigan, K. Lam, Matthew, Rheingold, L. Arnold, Inorg. Chem. 41 (2002) 1030–1032.
[14] J. Liang, Y. Wang, J.H. Yu, Y. L., R.R. Xu, Chem. Commun. (2003) 882–883.
[15] R.P. Doyle, M. Nieuwenhuyzenc, P.E. Kruger, Dalton Trans. (2005) 3745–3750.
[16] G.M. Sheldrick, SHEXTL-97, Programs for Crystal Structure Refinements, University of Göttingen, Germany, 1997.
[17] S. Bordiga, C. Lamberti, G. Ricchiardi, L. Regli, F. Bonino, A. Damin, K.P. Lillerud, M. Bjorgen, A. Zecchina, Chem. Commun. (2004) 2300–2301.
[18] F. Wang, K.A. Berglund, Ind. Eng. Chem. Res. 39 (2000) 2101–2104.
[19] S. Randy Jr., L. Rarig, Y. Robert, Peter Zavalij, N.J. Katana, L. Robert, Jr. LaDuca, Greedan, E. John, Z. Jon, Inorg. Chem. 41 (2002) 2124–2133.
[20] C. Robert, R.S. Finn Jr., Rarig, J. Zubieta, Inorg. Chem. 41 (2002) 2109–2123.
[21] A. Ponnaiyan, E. Owen, R.M. Bruce, Foxman, A.K. Wheeler, H. Timothy, j. Warren, L.W. bin, Inorg. Chem. 40 (2001) 5954–5961.
[22] J.Y. Niu, J.P. Wang, Introduction of Heteropoly Compounds, Henan University Press, Kaifeng, 2000.
[23] X.M. Lin, L. Chen, H.C. Fang, Z.Y. Zhou, X.X. Zhou, J.Q. Chen, W. Xu, Y.P. Cai, Inorg. Chim. Acta 362 (2009) 2619–2626.
[24] H.N. Wang, J.S. Qin, D.Y. Du, G.J. Xu, X.L. Wang, K.Z. Shao, G. Yuan, L.J. Li, Z.M. Su, Inorg. Chem. Commun. 13 (2010) 1227–1230.
[25] Y.Q. Lan, S.L. Li, X.L. Wang, K.Z. Shao, Z.M. Su, E.B. Wang, Inorg. Chem. 47 (2008) 529–534.